POLITECNICO DI TORINO
Repository ISTITUZIONALE

Impact of Dzyaloshinskii-Moriya interactions on the thermal stability factor of heavy metal/magnetic metal/oxide based nano-pillars

(Article begins on next page)

28 April 2024

Impact of Dzyaloshinskii-Moriya interactions on the thermal stability factor of heavy metal/magnetic metal/oxide based nano-pillars

Daniele Gastaldo (iD), Nikita Strelkov (iD), Liliana D. Buda-Prejbeanu (iD), Bernard Dieny (iD), Olivier Boulle (iD), Paolo Allia (iD), and Paola Tiberto

View Online   Export Citation   CrossMark

ARTICLES YOU MAY BE INTERESTED IN

Impact of Dzyaloshinskii-Moriya interactions on the thermal stability factor of heavy metal/magnetic metal/oxide based nano-pillars

View Online   Export Citation   CrossMark

Daniele Gastaldo,[1,2,a)] (iD) Nikita Strelkov,[3,4] (iD) Liliana D. Buda-Prejbeanu,[3] (iD) Bernard Dieny,[3] (iD) Olivier Boulle,[3] (iD) Paolo Allia,[2] (iD) and Paola Tiberto[2]

AFFILIATIONS

[1]Applied Science and Technology Department (DiSAT), Politecnico di Torino, corso Duca degli Abruzzi 24, 10129 Turin, Italy
[2]Advanced Materials Metrology and Life Sciences Division, Istituto Nazionale di Ricerca Metrologica (INRiM), Strada delle Cacce 91, 10135 Turin, Italy
[3]Université Grenoble Alpes, CEA, CNRS, Grenoble INP, IRIG-SPINTEC, 17 rue des Martyrs, 38054 Grenoble Cedex 9, France
[4]Department of Physics, Moscow Lomonosov State University, Moscow 119991, Russia

[a)]**Electronic mail:** daniele.gastaldo@polito.it

ABSTRACT

We studied the thermal stability of ultrathin perpendicular magnetized nanodots in the presence of the Dzyaloshinskii-Moriya interaction (DMI) using a minimum energy path method. We find that the smallest energy barrier is associated with the energy path based on domain wall nucleation and propagation down to 25 nm lateral size. We show that the DMI has a detrimental impact on the thermal stability factor of square $Pt/Co/AlO_x$ dots, which decreases linearly with the DMI amplitude. Our study reveals that the DMI limits the downscaling of MRAM cells based on heavy metal/ferromagnet/oxide trilayers.

Published under license by AIP Publishing. https://doi.org/10.1063/1.5109484

I. INTRODUCTION

Many theoretical and experimental studies have focused on improving performances of thin-film systems exhibiting strong perpendicular magnetic anisotropy (PMA) because of their potential integration in spintronic devices (e.g., magnetic random-access memory, racetrack memory,[1] nonvolatile logic circuits,[2] and field sensors). This perpendicular anisotropy originates at the interfaces of the ferromagnetic (FM) layer (e.g., Fe, Co, and CoFeB) due to spin orbit coupling and interfacial orbital hybridization.[3–5] This is particularly the case at FM/oxide (e.g., AlO and MgO) or FM/heavy metal (e.g., Pt and Ta) interfaces. The interfacial anisotropy competes with the bulk shape anisotropy and leads, for sufficiently thin FM layers (thickness typically below 1.4 nm),[6] to a preferential orientation of the magnetization perpendicular to the plane of the layers. Thus, two magnetic states can be stabilized at a zero applied field (magnetization up and down) useful to code binary information (0 and 1) in a magnetic random-access memory cell (MRAM). Key parameters for a nonvolatile memory application are write endurance, power consumption, and data retention. A good trade-off among them must be found in order to compete efficiently with alternative technologies. The efforts in spintronics are now concentrated on two families of MRAMs: spin-transfer torque (STT[7]) and spin-orbit torque (SOT[8]), named after their writing principle. Both comprise a very thin ferromagnetic storage layer with interfacial perpendicular anisotropy. The phenomena acting at interfaces are not only creating the magnetic anisotropy but are also known to generate additional interactions such as chiral exchange[9–12] or damping enhancement[13] with a strong impact on the static and dynamic properties of the storage layer. Particularly, the interfacial Dzyaloshinskii-Moriya interaction (DMI)[14,15] promotes states of noncollinear magnetization with an intrinsic tilt of magnetization at pillar edges,[16,17] stabilizes cycloidal states like chiral bubbles and skyrmions,[10,18] and assists fast magnetic domain wall (DW) motion.[19,20] Particularly, the creation and the manipulation of skyrmions (chiral bubbles) are mediated by the interfacial DMI, such spin structures being promising in view of conceiving various

applications.[21,22] Furthermore, several studies have already pointed out that interfacial DMI significantly reduces the current density required for magnetization switching in Pt/CoFeB/MgO trilayers,[23,24] but it also affects negatively the stability properties.

The aim of this work is, therefore, to understand whether and how much can the interfacial DMI either favor or be detrimental to the integration of Pt/Co/AlO$_x$ trilayers in memory devices. This trilayer structure has served as a model system to study the domain wall propagation under field and/or current in thin films or tracks[25,26] but also the magnetization reversal driven by spin-orbit torque in nanostructured square dots.[27] In this paper, we are interested in studying the thermal stability of the magnetization and its dependence on the lateral size of the nanostructure and the strength of the DMI. The present approach is based on a numerical micromagnetic approach. In the continuous approximation framework, considering the symmetry properties of Pt/Co/AlO, the interfacial Dzyaloshinskii-Moriya interaction contribution to exchange can be rewritten in terms of an energy density as[19]

$$\varepsilon_{DMI} = D\big(m_z\partial_x m_x - m_x\partial_x m_z + m_z\partial_y m_y - m_y\partial_y m_z\big), \quad (1)$$

where **m** is the unitary vector of the magnetization and D is a continuous effective DMI parameter. The value of D can be derived from an atomistic description depending on the crystal symmetry, the thickness of the ferromagnetic film, and the nature of the interfaces. For a thin film of thickness t having a simple cubic structure with constant a, D scales with $d/(at)$,[17] where d is the amplitude of DMI interaction between atomic nearest neighbors. The z-axis is the vertical axis which coincides with the structural inversion asymmetry axis of the trilayer structure, while x and y are, respectively, the planar axes. The thermal stability factor is defined as the ratio $\Delta = E_B/(k_B T)$ which enters into an Arrhenius type law governing the transition rate $P(T) = f_0 e^{-E_B/k_B T}$, with f_0 being the attempt frequency (1 GHz). Here, E_B is the activation energy and $k_B T$ is the thermal activation energy with k_B Boltzmann's constant, and T is the operating temperature. The activation energy E_B characterizes a strong, exponential dependence of the lifetime with temperature, and its estimation gives direct access to the stability. In the data storage industry, for the magnetic media of hard disk drives, the thermal stability factor is usually tuned above $42 k_B T$ to insure 10 years of stability of the recorded information. For memory applications like MRAMs, the requirements are more severe since it concerns large arrays of memory cells. The failure rate in standby combines both the thermal stability factor Δ and the capacity of the array. The higher the memory capacity, the larger the thermal stability for a given probability of failure in time (e.g., an areal density of 1 Gb requests above $70 k_B T$[28]). The thermal stability factor also determines the probability of the read disturb error (write error while reading) due to the STT produced by the read current in STT or SOT-MRAM.[28]

II. NUMERICAL METHOD

To estimate the stability factor Δ, a micromagnetic approach based on the string method (minimum energy path, MEP)[29,30] has been used. This technique allows one to explore the energy landscape of the sample to identify the most probable path which is

taken by the system (spontaneously) from the initial state to the final state. The numerical implementation consists of two steps. The first step allows finding the initial and final magnetization stable states between which the system might commute spontaneously. To this aim, the Landau-Lifshitz-Gilbert (LLG) equation has been numerically solved using the Micro3D solver including the DMI contribution [Eq. (1)],[31] this step is a usual energy minimization procedure. In the second step, a string approach to find the MEP between these two stable states has been developed.[32–36] Thus, a set of intermediate states has been considered (e.g., initial guessed path having 50 frames). Afterward, all the intermediate states are let to evolve following the overdamped LLG equation (damping $\alpha = 0.5$) until a user-selected time interval has elapsed (e.g., $\tau = 50$ ps), allowing the energy landscape to be progressively explored. Subsequently, an interpolation procedure has been applied to the intermediate states in order to construct a path in the system phase diagram between the initial and final states; this reparametrization being required to keep these intermediate states equidistant. The evolution of the intermediate states and their interpolation have been repeated until the maximum relative energy error on the last interpolated MEP path is less than a user-selected numerical tolerance (in this work, 10^{-5}). The above described procedure has been successfully applied to analyze the thermal stability factor of perpendicular shape anisotropy STT-MRAM cells.[37] Our samples are square dots of Pt/Co/AlO$_x$ with a Co layer of 0.6 nm and various lateral sizes. The following parameters have been used for Co:[38] a saturation magnetization of $M_s = 1.09$ kA/m, a uniaxial anisotropy constant of $K_u = 1.25e6$ J/m^3, an exchange stiffness of $A_{ex} = 10$ pJ/m, and a Gilbert damping parameter of $\alpha = 0.5$. The simulations were
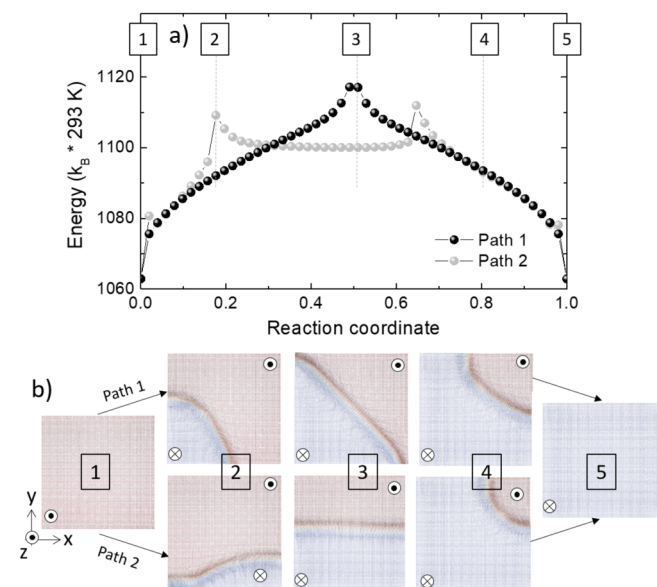

FIG. 1. (a) MEP converged paths for two initial guessed paths in a 100 nm lateral size Co dot with $D = 2$ mJ/m^2. (b) The corresponding snapshots of the magnetization distribution at different reaction coordinates: initial (1), intermediate (2, 3, and 4), and final (5).
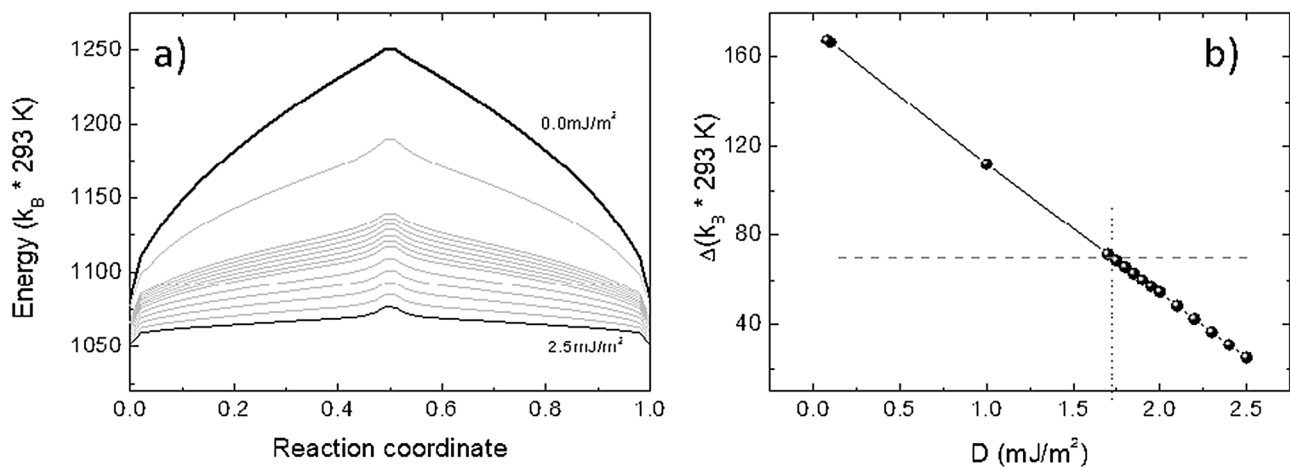
FIG. 2. (a) Evolution of the MEP with the D value in the range $0.0-2.5\,\text{mJ/m}^2$ for a 100 nm wide square dot. (b) Variation of the thermal stability factor Δ with D estimated at room temperature. The gray dotted line indicates the $70k_BT$ threshold.

performed at zero absolute temperature ($T = 0\,\text{K}$) using a maximum mesh size of 1 nm. These values of the material parameters allow for a single domain state (perpendicularly magnetized up or down) at zero applied field and they have been set in agreement with our previous study.[39] It is possible to vary these values as far as the stable states mentioned above are not affected. In the present study, we are focusing on the role played by the DMI; thus different values of the DMI constant were used keeping unchanged the other parameters.

III. SIMULATIONS RESULTS

As a general feature, with very few exceptions, several energy barriers can separate the two stable states, this is the reason why several initial guessed paths have been tested and compared looking to find the smallest activation energy value. Figure 1 shows the results of a typical MEP simulation for two selected initial guessed paths (i.e., coherent rotation of the magnetization and Bloch DW nucleation and propagation) for a 100 nm lateral size square dot. The two equilibrium states labeled (1) and (5) in Fig. 1(b) correspond to average magnetization pointing up (along the $+Oz$ axis) or down ($-Oz$), respectively, and they are stable in zero applied field. The magnetization at the edges of the dot is tilted under the effect of the DMI of constant $D = 2\,\text{mJ/m}^2$, with a maximum angle of about $31°$. Both paths converge toward mechanisms based on nucleation and propagation of a magnetic domain wall. As expected, since there in no applied field to break the symmetry, the up-down
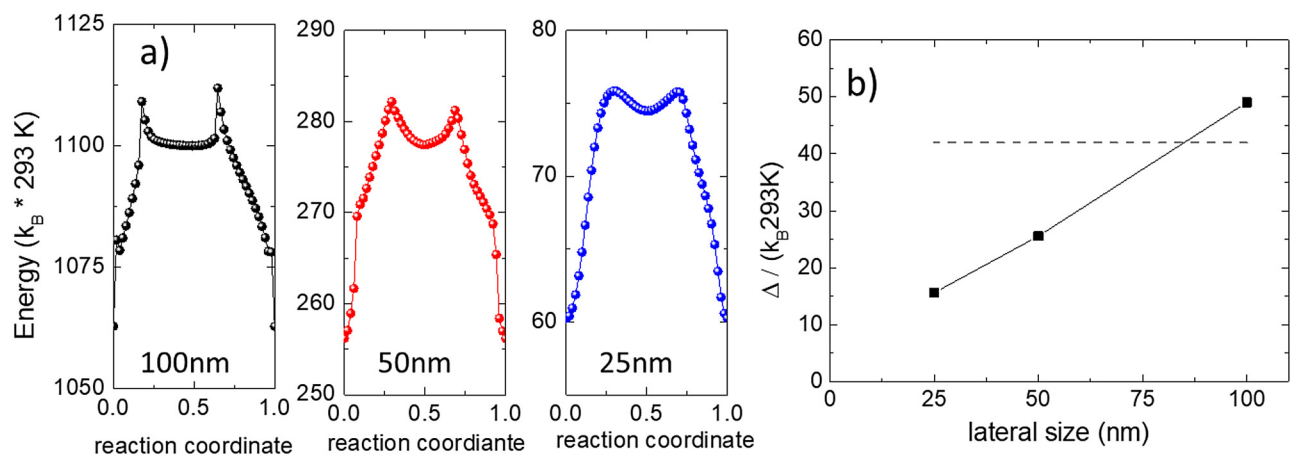

FIG. 3. (a) MEP profile for 100 nm (black), 50 nm (red), and 25 nm (blue) lateral size dots with $D = 2\,\text{mJ/m}^2$. (b) Thermal stability factor Δ as a function of the lateral size L estimated at room temperature. The gray dotted line indicates the $42k_BT$ threshold.

and down-up magnetization commutations are equivalent in terms of activation energy. However, the solutions are distinct since the energy variation along the reaction coordinate presents one maximum for path 1 and two maxima for path 2. The first solution predicts a DW nucleation at a corner of the sample, propagation along the diagonal of the square and expulsion at the opposite corner. Instead for path 2, even if the DW nucleation still occurs at a corner of the sample, the DW deviates from the diagonal.

At point (3), the DW realigns with the edge of the square, thus generating a local minimum in the energy profile. However, the internal structure of the domain wall corresponds to a Néel type as expected for a left-handed DMI interaction.[25] Several other initial guessed paths were tested (e.g., intermediate frames with random distribution of the magnetization) but the lowest energy MEPs identified for this set of material parameters are these two solutions.

For this reason, the analysis will be hereafter continued using these solutions but varying both the sample size and the DMI value.

Figure 2 reports the dependence of the MEP profile of the first solution (single barrier profile) upon varying the strength of the DMI from 0 to 2.5 mJ/m², a range for which the states with magnetization up and down are stable states. Qualitatively, we observed that an increase in DMI shifts the MEP profiles toward lower energies [Fig. 2(a)] with a negligible impact on the shape of the profiles. This trend is confirmed by Fig. 2(b), which shows the evolution of the thermal stability factor Δ with the D parameter at room temperature. It turns out that the thermal stability factor Δ is linearly decreasing with DMI strength. This result can be understood by analyzing the DMI contribution to DW energy since the switching mechanism is based on DW nucleation and propagation. The DW energy per unit surface for a ferromagnet magnetized out of plane varies linearly with the DMI value according to the relation $\sigma = 4\sqrt{(A_{ex}(K_u - \mu_0 M_s^2/2))} - \pi D$ for our left-handed Neel domain wall.[17] This means that the energy of the DW decreases upon reinforcing the DMI and thus favoring the nucleation of a DW. As a partial conclusion, one might notice that the 100 nm wide Co square dot represents the $70k_BT$ threshold if the DMI is below 1.7 mJ/m². One might note that the DW energy depends on the saturation magnetization, the anisotropy, as well as the exchange stiffness. The results of our study will be still valid if these parameters are modified, for example, the energy of the DW stays positive.

The thermal stability factor is expected to vary with the sample volume since the latter is involved in the height of the energy barrier E_B. Hereafter, we have performed simulations by varying dots lateral dimension in the range 25 nm–100 nm at a constant D value. As shown in Fig. 3(a), the shape of the MEP profiles (solution 2 having 2 local maxima) evolves slightly with the lateral size of the dot while the curves are shifted downward toward lower energy upon reducing the sample volume. The thermal stability factor was found to increase almost linearly with the lateral size [Fig. 3(b)], not with the dotted area for a given thin film thickness. This can be explained by the fact that the energy barrier is essentially proportional to the DW length, which scales like the cell size since the domain wall extends between two parallel sides of the dot at the top of the MEP profiles.[40] The DMI value of 2 mJ/m² has been chosen on purpose, in agreement with the previous estimated value for Pt/Co/metal oxide systems.[41] For

such a moderate to large DMI interaction, the predicted thermal stability factor appears to be well below the $70k_BT$ threshold and it goes even below the limit of $42k_BT$. In conclusion, the DMI interaction imposes a bottom limit size for the cell and should be carefully considered in the design of dense MRAM arrays. For the particular case of a cell based on Pt/Co(0.6 nm)/AlO$_x$, the lateral size of the dot should be above 100 nm, this value being detrimental for use in compact and dense memories.

The reduction in the size of the dot has not only the consequence of reducing the thermal stability factor Δ but also the one
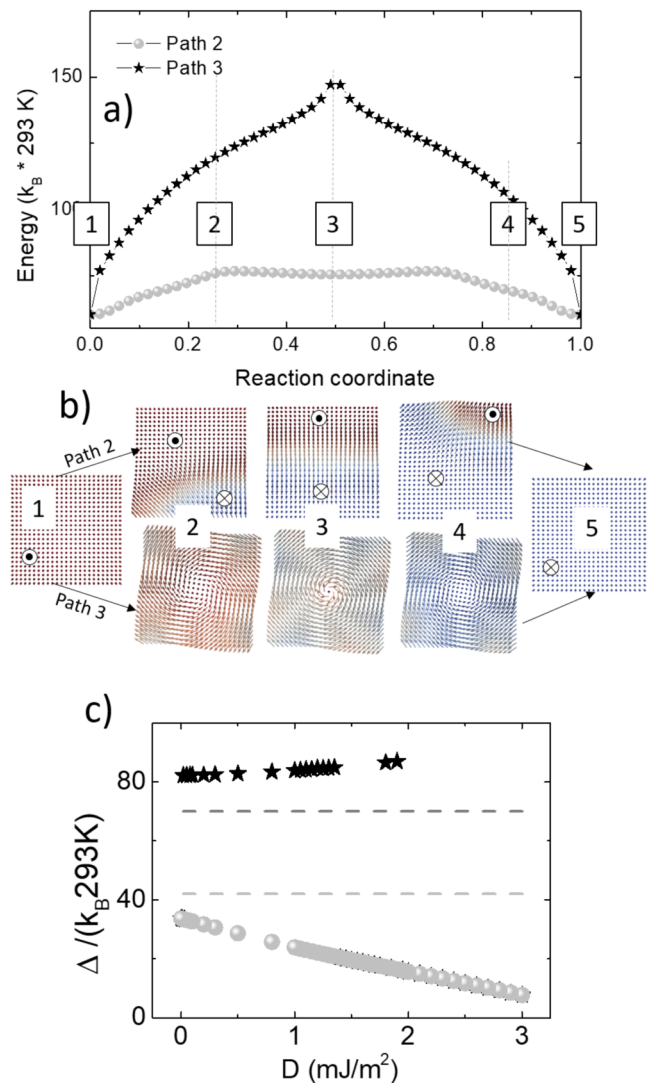

FIG. 4. (a) MEP converged paths of a 25 nm lateral size dot labeled path 1 and path 3 ($D = 2$ mJ/m²). (b) The corresponding snapshots of the magnetization distribution at different reaction coordinates: initial (1), intermediate (2, 3, and 4), and final (5). (c) Thermal stability factor as a function of the DMI strength D estimated at room temperature.

of modifying the switching paths obtained by MEP simulations. In fact, for smaller dots (lateral dimensions equal to 25 nm), MEP solution 1 obtained from the initial guessed path based on coherent rotation (path 1) is no longer accessible as in the case of the larger dots. The symmetry of solution 3 is very similar to that of solution 1 as shown in Fig. 4(a). However, such a third solution is based on quasicoherent spin rotation, like magnetization curling, as indicated by the bottom line of snapshots in Fig. 4(b). In contrast with the previous two solutions (1 and 2), the thermal stability factor Δ of the third solution is quite large (above $70k_BT$) even at very high DMI. This is indicative of the fact that the mechanism behind this type of commutation is highly energetic since it involves a confinement of spin texture in the center of the dot (intermediate snapshot 3) concentrating a large amount of exchange and DMI energy in a very small volume. One positive feature of this solution is that the DMI interaction is not reducing anymore the associated thermal stability factor but even slightly increases it [Fig. 4(c)]. However, this apparent advantage has no impact on the effective thermal stability factor as determined by solution 2, because the system evolution will always follow the path with the lowest energy barrier E_B.

IV. CONCLUSIONS

In conclusion, we have shown that the interfacial Dzyaloshinskii-Moriya has a detrimental impact on the thermal stability factor of square dots Pt/Co/AlO$_x$. The activation energy E_B in such thin ferromagnetic layers with strong out-of-plane anisotropy is associated with MEP solutions based on domain wall nucleation and propagation. This mechanism is valid for lateral sizes down to 25 nm. Upon increasing the interfacial DMI, the thermal stability factor is linearly decreasing because of the chiral DW energy linear reduction with the DMI. With the parameters used, our study reveals that tailoring MRAM cells based on the HM/FM/oxide trilayer would limit downscaling. To overcome the detrimental impact of the DMI on the stability, technological solution based on the reinforcing of the anisotropies of the storage (magnetocrystalline and/or shape) should be considered.

SUPPLEMENTARY MATERIAL

See the supplementary material for videos of the 3 MEP simulated switching solutions.

ACKNOWLEDGMENTS

REFERENCES

[1]S. S. P. Parkin, M. Hayashi, and L. Thomas, Science **320**, 190 (2008).
[2]D. A. Allwood, Science **296**, 2003 (2002).
[3]S. Peng, M. Wang, H. Yang, L. Zeng, J. Nan, J. Zhou, Y. Zhang, A. Hallal, M. Chshiev, K. L. Wang, Q. Zhang, and W. Zhao, Sci. Rep. **5**, 18173 (2015).
[4]G. H. O. Daalderop, P. J. Kelly, and M. F. H. Schuurmans, Phys. Rev. B **50**, 9989 (1994).
[5]R. Wu and A. J. Freeman, J. Magn. Magn. Mater. **99**, 81 (1991).
[6]S. Ikeda, K. Miura, H. Yamamoto, K. Mizunuma, H. D. Gan, M. Endo, S. Kanai, J. Hayakawa, F. Matsukura, and H. Ohno, Nat. Mater. **9**, 721 (2010).
[7]B. Dieny and I. L. Prejbeanu, "Magnetic random access memory," in *Introduction to Magnetic Random Access Memory* (John Wiley & Sons, Ltd, 2016), Chap. 5, pp. 101–164.
[8]K. Garello, F. Yasin, S. Couet, L. Souriau, J. Swerts, S. Rao, S. V. Beek, W. Kim, E. Liu, S. Kundu, D. Tsvetanova, N. Jossart, K. Croes, E. Grimaldi, M. Baumgartner, D. Crotti, A. Furnémont, P. Gambardella, and G. Kar, in *2018 IEEE Symposium on VLSI Circuits Digest of Technical Papers* (IEEE, 2018).
[9]H. Sato, M. Yamanouchi, S. Ikeda, S. Fukami, F. Matsukura, and H. Ohno, Appl. Phys. Lett. **101**, 22414 (2012).
[10]A. Fert, V. Cros, and J. Sampaio, Nat. Nanotechnol. **8**, 152 (2010).
[11]M. Yamanouchi, L. Chen, J. Kim, M. Hayashi, H. Sato, S. Fukami, S. Ikeda, F. Matsukura, and H. Ohno, Appl. Phys. Lett. **102**, 212408 (2013).
[12]K. S. Ryu, L. Thomas, S. H. Yang, and S. Parkin, Nat. Nanotechnol. **8**, 527 (2013).
[13]P. J. Metaxas, J. P. Jamet, A. Mougin, M. Cormier, J. Ferré, V. Baltz, B. Rodmacq, B. Dieny, and R. L. Stamps, Phys. Rev. Lett. **99**, 217208 (2007).
[14]S. Heinze, K. Von Bergmann, M. Menzel, J. Brede, A. Kubetzka, R. Wiesendanger, G. Bihlmayer, and S. Blügel, Nat. Phys. **7**, 713 (2011).
[15]C. Moreau-Luchaire, C. Moutafis, N. Reyren, J. Sampaio, C. A. Vaz, N. Van Horne, K. Bouzehouane, K. Garcia, C. Deranlot, P. Warnicke, P. Wohlhüter, J. M. George, M. Weigand, J. Raabe, V. Cros, and A. Fert, Nat. Nanotechnol. **11**, 444 (2016); e-print arXiv:1502.07853.
[16]J. Sampaio, V. Cros, S. Rohart, A. Thiaville, and A. Fert, Nat. Nanotechnol. **8**, 839 (2013).
[17]S. Rohart and A. Thiaville, Phys. Rev. B **88**, 184422 (2013); e-print arXiv:1310.0666.
[18]N. Nagaosa and Y. Tokura, Nat. Nanotechnol. **8**, 899 (2013).
[19]A. Thiaville, S. Rohart, É. Jué, V. Cros, and A. Fert, Epl **100**, 57002 (2012); e-print arXiv:1211.5970.
[20]S. Emori, U. Bauer, S. M. Ahn, E. Martinez, and G. S. Beach, Nat. Mater. **12**, 611 (2013); e-print arXiv:1302.2257.
[21]W. Jiang, W. Zhang, M. B. Jungfleisch, F. Y. Fradin, J. E. Pearson, O. Heinonen, S. G. Te Velthuis, A. Hoffmann, P. Upadhyaya, G. Yu, K. L. Wang, and Y. Tserkovnyak, Science **349**, 283 (2015).
[22]G. Finocchio, G. Siracusano, R. Tomasello, A. Giordano, V. Puliafito, B. Azzerboni, O. Ozatay, and M. Carpentieri, Phys. Rev. Lett. **117**, 087204 (2016).
[23]P. H. Jang, K. Song, S. J. Lee, S. W. Lee, and K. J. Lee, Appl. Phys. Lett. **107**, 202401 (2015); e-print arXiv:1508.02587.
[24]J. Sampaio, A. V. Khvalkovskiy, M. Kuteifan, M. Cubukcu, D. Apalkov, V. Lomakin, V. Cros, and N. Reyren, Appl. Phys. Lett. **108**, 112403 (2016); e-print arXiv:1601.00598.
[25]S. Pizzini, J. Vogel, S. Rohart, L. Buda-Prejbeanu, E. Jué, O. Boulle, I. Miron, C. Safeer, S. Auffret, G. Gaudin, and A. Thiaville, Phys. Rev. Lett. **113**, 047203 (2014).
[26]E. Jué, C. K. Safeer, M. Drouard, A. Lopez, P. Balint, L. Buda-Prejbeanu, O. Boulle, S. Auffret, A. Schuhl, A. Manchon, I. M. Miron, and G. Gaudin, Nat. Mater. **15**, 272 (2016); e-print arXiv:1504.04411v1.
[27]K. Garello, C. O. Avci, I. M. Miron, M. Baumgartner, A. Ghosh, S. Auffret, O. Boulle, G. Gaudin, and P. Gambardella, Appl. Phys. Lett. **105**, 30 (2014); e-print arXiv:1310.5586.
[28]B. Dieny and M. Chshiev, Rev. Mod. Phys. **89**, 025008 (2017).
[29]E Weinan, W. Ren, and E. Vanden-Eijnden, J. Chem. Phys. **126**, 164103 (2007).
[30]P. F. Bessarab, V. M. Uzdin, and H. Jónsson, Comput. Phys. Commun. **196**, 335 (2015); e-print arXiv:1502.05065.
[31]L. Buda, I. Prejbeanu, U. Ebels, and K. Ounadjela, Comput. Mater. Sci. **24**, 181 (2002).
[32]H. Forster, N. Bertram, X. Wang, R. Dittrich, and T. Schrefl, J. Magn. Magn. Mater. **267**, 69 (2003).
[33]W. E, W. Ren, and E. Vanden-Eijnden, Phys. Rev. B **66**, 052301 (2002).

[34]E. Weinan, W. Ren, and E. Vanden-Eijnden, J. Appl. Phys. **93**, 2275 (2003).

[35]M. F. Carilli, K. T. Delaney, and G. H. Fredrickson, J. Chem. Phys. **143**, 054105 (2015).

[36]G. D. Chaves-O'Flynn, D. Bedau, E. Vanden-Eijnden, A. D. Kent, and D. L. Stein, IEEE Trans. Magn. **46**, 2272 (2010).

[37]N. Perrissin, S. Lequeux, N. Strelkov, A. Chavent, L. Vila, L. D. Buda-Prejbeanu, S. Auffret, R. C. Sousa, I. L. Prejbeanu, and B. Dieny, Nanoscale **10**, 12187 (2018); e-print arXiv:1803.02663.

[38]I. M. Miron, T. Moore, H. Szambolics, L. D. Buda-Prejbeanu, S. Auffret, B. Rodmacq, S. Pizzini, J. Vogel, M. Bonfim, A. Schuhl, and G. Gaudin, Nat. Mater. **10**, 419 (2011).

[39]N. Mikuszeit, O. Boulle, I. M. Miron, K. Garello, P. Gambardella, G. Gaudin, and L. D. Buda-Prejbeanu, Phys. Rev. B **92**, 1 (2015).

[40]D. Apalkov, B. Dieny, and J. Slaughter, Proc. IEEE **104**, 1796 (2016).

[41]H. Yang, O. Boulle, V. Cros, A. Fert, and M. Chshiev, Sci. Rep. **8**, 1 (2018); e-print arXiv:1603.01847.